NASA/TM—2012-217674 AIAA–2012–2252

# Acoustic Measurements of Rectangular Nozzles With Bevel

*James E. Bridges*
*Glenn Research Center, Cleveland, Ohio*

August 2012

# NASA STI Program . . . in Profile

Since its founding, NASA has been dedicated to the advancement of aeronautics and space science. The NASA Scientific and Technical Information (STI) program plays a key part in helping NASA maintain this important role.

The NASA STI Program operates under the auspices of the Agency Chief Information Officer. It collects, organizes, provides for archiving, and disseminates NASA's STI. The NASA STI program provides access to the NASA Aeronautics and Space Database and its public interface, the NASA Technical Reports Server, thus providing one of the largest collections of aeronautical and space science STI in the world. Results are published in both non-NASA channels and by NASA in the NASA STI Report Series, which includes the following report types:

- TECHNICAL PUBLICATION. Reports of completed research or a major significant phase of research that present the results of NASA programs and include extensive data or theoretical analysis. Includes compilations of significant scientific and technical data and information deemed to be of continuing reference value. NASA counterpart of peer-reviewed formal professional papers but has less stringent limitations on manuscript length and extent of graphic presentations.

- TECHNICAL MEMORANDUM. Scientific and technical findings that are preliminary or of specialized interest, e.g., quick release reports, working papers, and bibliographies that contain minimal annotation. Does not contain extensive analysis.

- CONTRACTOR REPORT. Scientific and technical findings by NASA-sponsored contractors and grantees.

- CONFERENCE PUBLICATION. Collected papers from scientific and technical conferences, symposia, seminars, or other meetings sponsored or cosponsored by NASA.

- SPECIAL PUBLICATION. Scientific, technical, or historical information from NASA programs, projects, and missions, often concerned with subjects having substantial public interest.

- TECHNICAL TRANSLATION. English-language translations of foreign scientific and technical material pertinent to NASA's mission.

Specialized services also include creating custom thesauri, building customized databases, organizing and publishing research results.

For more information about the NASA STI program, see the following:

- Access the NASA STI program home page at *http://www.sti.nasa.gov*

- E-mail your question to *help@sti.nasa.gov*

- Fax your question to the NASA STI Information Desk at 443–757–5803

- Phone the NASA STI Information Desk at 443–757–5802

- Write to:
  STI Information Desk
  NASA Center for AeroSpace Information
  7115 Standard Drive
  Hanover, MD 21076–1320

NASA/TM—2012-217674 AIAA–2012–2252

# Acoustic Measurements of Rectangular Nozzles With Bevel

*James E. Bridges*
*Glenn Research Center, Cleveland, Ohio*

Prepared for the
18th Aeroacoustics Conference
cosponsored by the American Institute of Aeronautics and Astronautics and
the Confederation of European Aerospace Societies
Colorado Springs, Colorado, June 4–6, 2012

National Aeronautics and
Space Administration

Glenn Research Center
Cleveland, Ohio 44135

August 2012

**Acknowledgments**

The Supersonics Project of the NASA Fundamental Aeronautics Program supported this work. The author gratefully acknowledges the work of Franco Frate in creating these nozzles, and of Milo Dahl and Jeff Berton in giving the manuscript a thorough thrice-over.



This work was sponsored by the Fundamental Aeronautics Program at the NASA Glenn Research Center.

*Level of Review*: This material has been technically reviewed by technical management.

Available from

NASA Center for Aerospace Information
7115 Standard Drive
Hanover, MD 21076–1320

National Technical Information Service
5301 Shawnee Road
Alexandria, VA 22312

Available electronically at http://www.sti.nasa.gov

# Acoustic Measurements of Rectangular Nozzles With Bevel

James E. Bridges
National Aeronautics and Space Administration
Glenn Research Center
Cleveland, Ohio 44135

## Abstract

A series of convergent rectangular nozzles of aspect ratios 2:1, 4:1, and 8:1 were constructed with uniform exit velocity profiles. Additional nozzles were constructed that extended the wide lip on one side of these nozzles to form beveled nozzles. Far-field acoustic measurements were made and analyzed, and the results presented. The impact of aspect ratio on jet noise was similar to that of enhanced mixing devices: reduction in aft, peak frequency noise with an increase in broadside, high frequency noise. Azimuthally, it was found that rectangular jets produced more noise directed away from their wide sides than from their narrow sides. The azimuthal dependence decreased at aft angles where noise decreased. The effect of temperature, keeping acoustic Mach number constant, was minimal. Since most installations would have the observer on the wide size of the nozzle, the increased high frequency noise has a deleterious impact on the observer. Extending one wide side of the rectangular nozzle, evocative of an aft deck in an installed propulsion system, increased the noise of the jet with increasing length. The impact of both aspect ratio and bevel length were relatively well behaved, allowing a simple bilinear model to be constructed relative to a simple round jet.

### Nomenclature

| | |
|---|---|
| *AR* | aspect ratio |
| $a_j$ | speed of sound in jet fluid, exit conditions |
| $a_\infty$ | speed of sound in ambient |
| *a* | coefficient of model fit corresponding to aspect ratio |
| *b* | coefficient of model fit corresponding to bevel length |
| *c* | coefficient of model fit corresponding to interaction of aspect ratio and bevel length |
| $D_e$ | diameter, equivalent area |
| *f* | frequency |
| *h* | short dimension of rectangular nozzle exit |
| *L* | length of bevel beyond exit of baseline nozzle |
| *M* | jet aero Mach number, $U_j/a_j$ |
| *Ma* | acoustic Mach number, $U_j/a_\infty$ |
| *OASPL* | overall sound pressure level |
| *PSD* | power spectral density |
| *PSD*0 | spectral directivity of round jet |
| $T_j$ | jet static temperature, ideally expanded |
| $T_\infty$ | ambient temperature |
| $U_j$ | jet exit velocity, ideally expanded |
| $\theta$ | polar angle (fore to aft) |
| $\phi$ | azimuthal angle |

## 1.0 Introduction

The Supersonics Project of NASA’s Fundamental Aeronautics Program is developing technologies to enable civilian supersonic aircraft. Two of the top challenges to such vehicles have been sonic boom and noise around airports. One approach for reducing sonic boom is to avoid abrupt changes in aircraft cross-sectional area, hence embedding the propulsion. Also, for the propulsion system to vary its bypass ratio to meet both cruise performance and airport noise requirements requires nozzles with variable throat areas. Both of these aspects of supersonic aircraft design point to the need for non-axisymmetric inlets and nozzles. Many existing noise prediction tools explicitly assume axisymmetric nozzle geometry and should not predict noise accurately from such inlets and nozzles; others simply have not been tried to know if they work or not. As part of its exploration of nozzle concepts for quiet civilian supersonic aircraft, the NASA Supersonics Project created a family of high aspect ratio nozzles, the Extensible Rectangular Nozzles.

The initial goal of testing was to determine whether high aspect ratio nozzles showed promise for noise reduction, or conversely were louder than conventional nozzles, to gather basic noise data for creating empirical models, and to provide data for advanced noise prediction code development. The addition of such features as bevels and chevrons, present in current designs of military high aspect ratio nozzles, allows an initial assessment of their noise impact and challenges the high fidelity noise prediction tools being developed by and for NASA.

Preliminary design of the Extensible Rectangular Nozzle (ERN) model system was started in June 2007 and initial flow lines were worked out using RANS CFD in 2009. In November 2009, the design was redirected to a smaller scale rig and mechanical design of the basic test articles was completed by March 2010. Final flow lines of all concepts were analyzed using RANS CFD before the model system was fabricated, which occurred from June to November 2010. Reference 1 gives a full account of the results of these analyses. The models were tested for far-field noise in December 2010. This document analyzes the results of this acoustic test.

A few other researchers have investigated rectangular nozzles previously. One example is the work of General Electric Co., who acquired data at a jet rig at their Corporate Research and Development labs in the late 1970’s. Figure 1 is from a report (Ref. 2) generated for FAA showing their outdoor hot jet rig. One aspect ratio, 6:1, was tested on the rig, which was also used for testing twin jets, hence the multi-flanged plenum. In another example of previous work, Georgia Tech Research Institute (GTRI) made a more thorough investigation (Ref. 3) of rectangular nozzle, pictured in Figure 2. This report gives results for aspect ratios 1.5, 4, and 8. Results from these previous tests will be compared with the current test results in the Analysis section of this paper.

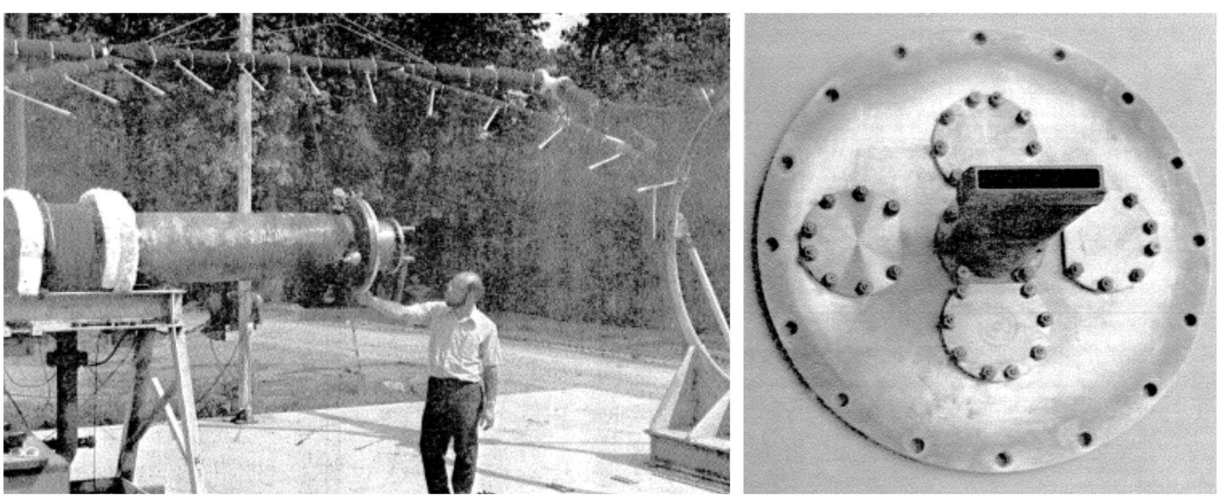

Figure 1.—Jet facility at General Electric and 6:1 nozzle, documented in Reference 2.

Figure 2.—Round and rectangular nozzles used in GTRI study, Reference 3.

## 2.0 Facility, Model Hardware, Instrumentation, and Flow Conditions

The test was conducted on the Small Hot Jet Acoustic Rig (SHJAR, pronounced with a silent ‘J’) , shown in Figure 3. The rig is located in the Aero-Acoustic Propulsion Laboratory (AAPL) at the NASA Glenn Research Center in Cleveland, Ohio. The SHJAR was developed to test jet noise reduction concepts at a low technology readiness level (TRL 1-3) and at minimum expense. The AAPL, which houses the SHJAR, is a geodesic dome (60-ft radius) lined with sound-absorbing wedges which reduce sound reflection at all frequencies above 200 Hz.

Acoustic measurements were made on an arc of constant 150-in. (3.81 m) radius from the jet exit centerline. The 24 microphones spaced at 5° increments afforded a range of polar angles from 50° to 165° relative to the upstream jet axis. Signals from the ¼ in. Bruel & Kjaer 3943 microphones were run through Bruel & Kjaer NEXUS signal conditioners before being recorded for later narrowband analysis. Simultaneously with the acoustic recording, the ambient temperature, pressure, and relative humidity were also recorded, allowing for accurate reinstatement of the atmospheric attenuation suffered by the high frequencies of the signal. The flow setpoints were defined by acoustic Mach number (velocity relative to ambient speed of sound) and static temperature ratio. These values were maintained within 0.5 percent cumulative for all acquisitions. This is an important point given that rotating the nozzle and repeating the test was done to obtain azimuthal variations in the sound field. Repeatability was found to be ±0.2 dB on a third octave basis.

As a jet noise test rig, the SHJAR was designed to minimize rig noise sources, incorporating the recommendations of Viswanathan (Ref. 4) and Ahuja (Ref. 5) to achieve this goal. The rig is a single flow jet rig that used 150-psi (1-MPa) air supplied by several remotely located compressors. The maximum mass flow rate was 6 lbm/sec (2.7 kg/s) and the maximum temperature air was 1300 °F (980 K). A hydrogen-fueled combustor permits a large range of temperature flows to be tested. The air passes through a baffled muffler and settling chamber before it reaches the nozzle. Two valves, a large main valve and a small vernier valve located upstream of the combustor and muffler, control the rate of airflow, providing fine control over the entire range of operating conditions. Flow conditions are measured in the 14 in. (356 mm) diameter plenum chamber located within the supporting frame. An ASME contraction connects the plenum chamber to a 6 in. (150 mm) diameter nozzle feedpipe that is 25 in. (635 mm) long. An extensive study of the acoustic properties of the SHJAR rig and its validation are given in Brown and Bridges (Ref. 6).

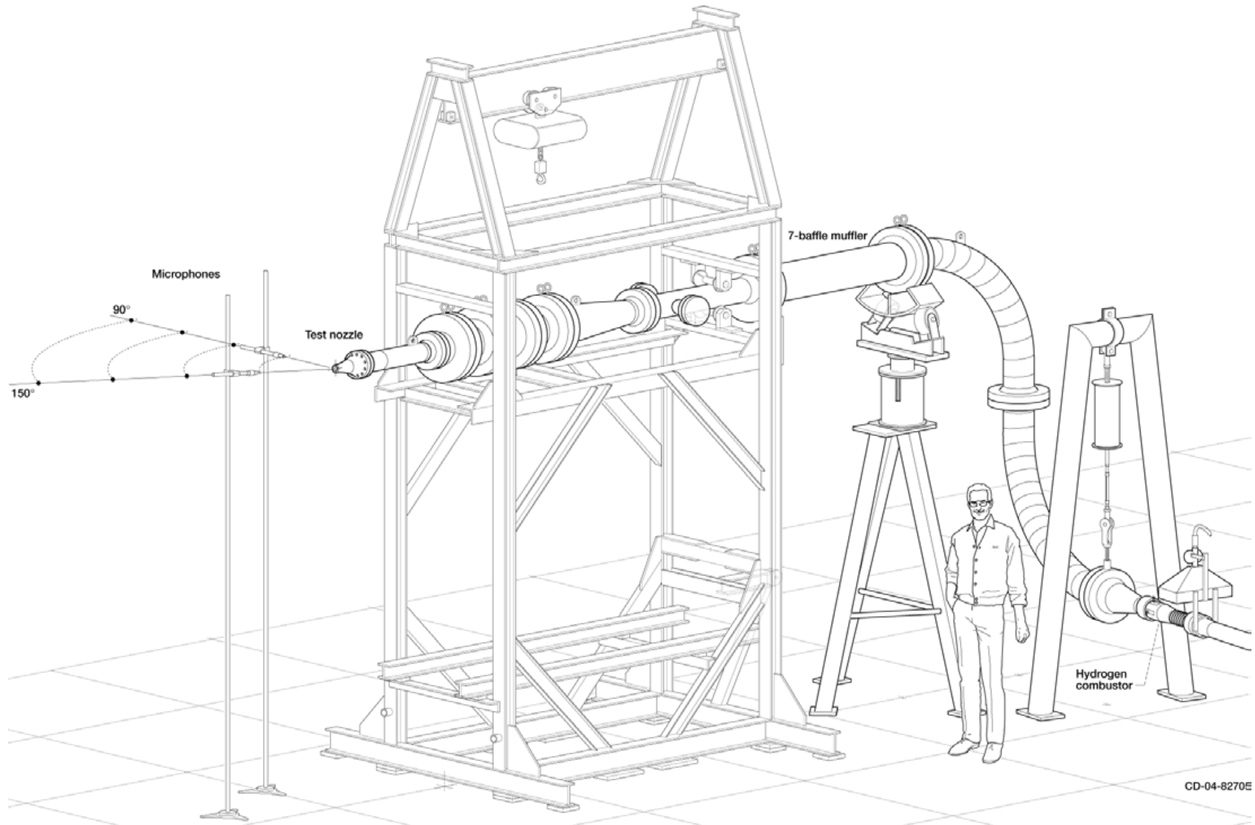


Figure 3.—Small Hot Jet Acoustic Rig (SHJAR) located at NASA Glenn's Aero-Acoustic Propulsion Laboratory.

The nozzles being tested were designed with a few criteria in mind. The key criteria were that the flow at the exit plane of the nozzle be uniform without swirl from the round-to-rectangular transition; that there be no separations on internal surfaces of the nozzles, that the nozzle lip be very thin to avoid lip-separation noise, and that the nozzles for a given aspect ratio have the same internal shape independent of the external features. The details of the design process, including CFD and mechanical stress analysis, are covered in the conference paper (Ref. 1).

The nozzles that were eventually fabricated for this test are shown graphically below in Table 1. From the top in the Table, three aspect ratios were chosen, 2:1, 4:1, and 8:1 with height *h* and width giving an equivalent diameter of 2.14 in. (545 mm). Beyond the basic rectangular nozzles, beveled designs with two different extension lengths *L* were explored for each aspect ratio. The lengths of the lower edge of beveled nozzle were made in increments relative to the minimum dimension of the rectangular nozzles, as given in Table 1. Other variations in nozzle design were constructed and tested, including chevrons on the wide sides of the rectangular nozzle, but these results will not be presented here for brevity.

Finally, as a reference, data were acquired with round nozzle of similar size (2 in. diameter) that has been tested extensively before (*cf.* Ref. 6; SMC000). Beyond being a reference for these rectangular nozzles, this allowed a check that the rig was performing as it has before.

To obtain the azimuthal dependence of the sound field with a single fixed microphone array the rig was shut down and the nozzle rotated to different azimuthal angles. Figure 4 shows the definitions of the polar and azimuthal angles used in these tests. With the basic rectangular nozzles a four-fold symmetry exists, but for the other nozzles only two-fold symmetry can be used. Data were acquired at 30° azimuthal increments for all geometries, this being sufficient to give a smooth variation in this coordinate. Because the test program had such a large number of geometries, and a large number of orientations for each of these geometries, only a cursory number of flow setpoints were explored.

TABLE 1.—DESIGN FEATURES OF NOZZLE HARDWARE

| | | |
|---|---|---|
| Basic nozzle, 2:1, 1.34- by 2.68-in. | NA2Z | 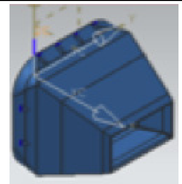 |
| Basic nozzle, 4:1, 0.948- by 3.79-in. | NA4Z | 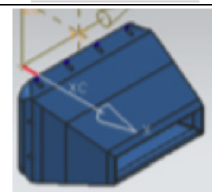 |
| Basic nozzle, 8:1, 0.671- by 5.36-in. | NA8Z | 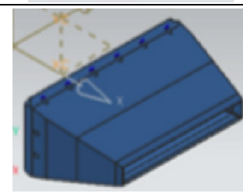 |
| Bevel nozzle, 2:1, 1.3 in. ext ($L/h$ = 1) | NA2B1 | 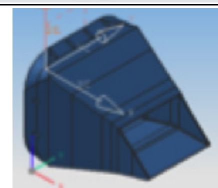 |
| Bevel nozzle, 2:1, 2.7 in. ext ($L/h$ = 2) | NA2B2 | 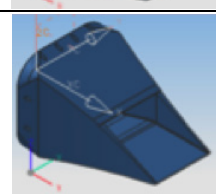 |
| Bevel nozzle, 4:1, 1.3 in. ext ($L/h$ = 1.4) | NA4B1 | 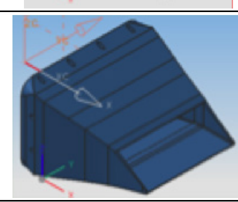 |
| Bevel nozzle, 4:1, 2.7 in. ext ($L/h$ = 2.8) | NA4B2 | 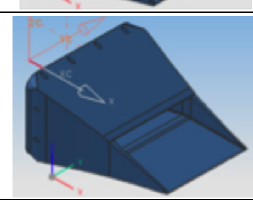 |
| Bevel nozzle, 8:1, 1.3 in. ext ($L/h$ = 2) | NA8B1 | 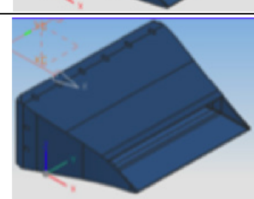 |
| Bevel nozzle, 8:1, 2.7 in. ext ($L/h$ = 4) | NA8B2 | 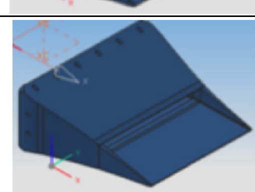 |

The flow setpoints were extracted from a much larger set that spans the range of velocity and temperatures previously tested on SHJAR for round and chevron nozzles, colloquially known as the Tanna matrix (Ref. 7). This subset was intended to minimally cover the subsonic and supersonic ranges, focusing on the high subsonic flows that are likely to be important in civilian supersonic aircraft. In addition, a few points were added to match on-going analysis by collaborators. Setpoints are defined in Table 2 by their acoustic Mach number *Ma* and their static temperature ratio $T_j/T_\infty$. Notes justify their inclusion. Hot flows were only acquired for a subset of geometries that first showed strong azimuthal variation in cold flow conditions and hence are not available for all configurations and azimuthal angles.

Far-field acoustic data presented below have been normalized by the nozzle equivalent diameter $D_e$ and the ideally expanded jet velocity $U_j$. Atmospheric attenuation has been added back to the spectra using Shields and Bass (Ref. 8), and spherical spreading assumption used to scale the data to an observer at 100 $D_e$. The units of the power spectral density (PSD) are 10log(Pa$^2$/St) dB reference to 20 µPa, where St = $fD_e/U_j$.

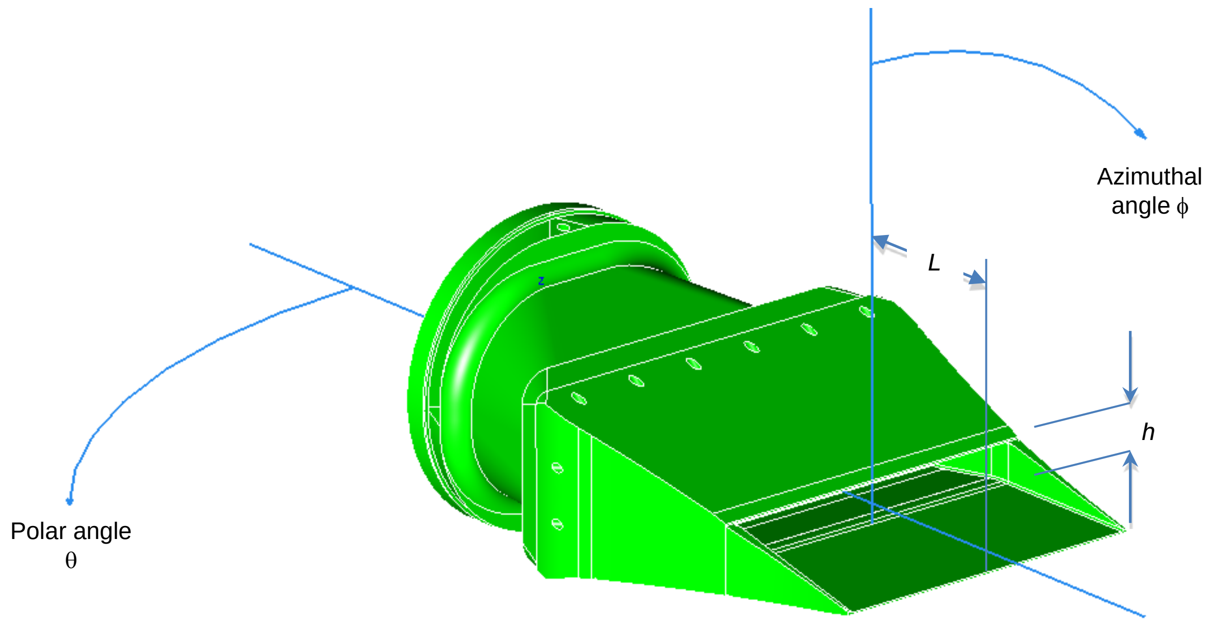


Figure 4.—Definition of azimuthal (ϕ) and polar (θ) angles and of bevel length *L* and nozzle height *h*.

TABLE 2.—FLOW CONDITION DEFINITIONS

| Setpoint | *Ma* | $T_j/T_\infty$ | *M* | Notes |
|---|---|---|---|---|
| | 0.50 | 0.95 | 0.51 | Tanna; low Ma |
| 5 | 0.70 | 0.90 | 0.74 | Tanna; low Ma |
| 7 | 0.90 | 0.84 | 0.98 | Tanna; high subsonic cold |
| 7010 | 0.95 | 0.80 | 1.05 | Slightly supersonic |
| 8010 | 1.05 | 0.78 | 1.18 | Supersonic |
| 9010 | 1.18 | 0.74 | 1.40 | Supersonic |
| 10010 | 1.25 | 0.69 | 1.50 | Supersonic |
| 23 | 0.50 | 1.76 | 0.38 | Tanna; low Ma warm |
| 27 | 0.90 | 1.76 | 0.68 | Tanna; high subsonic warm |
| 46 | 0.90 | 2.70 | 0.56 | Tanna; high subsonic hot |
| 29 | 1.33 | 1.76 | 1.01 | Tanna; v high subsonic warm |
| 48 | 1.33 | 2.70 | 0.82 | Tanna; v high subsonic hot |

# 3.0 Results

## 3.1 Basic Results

For this paper, a representational subset of the data will be presented and the presentation will start with overall sound pressure level (OASPL) as a function of azimuthal and polar angles. The OASPL directivity for basic rectangular nozzles operating cold at acoustic Mach number 0.9 is given in Figure 5. For this flow condition the 2:1 aspect ratio shows very little difference from a round jet for polar angles 90° < θ < 140°. There are some variations at upstream angles that are not monotonic in azimuthal angle, and a more systematic variation at the far aft angles (θ > 150°). The 4:1 jet shows a stronger variation over polar angles greater than 90°, with variations up to 2 dB with azimuthal angle, and the 8:1 jet even more so with variations up to 3 dB. The 4:1 and 8:1 have similar trends with both polar and azimuthal angle. Far aft angles (θ > 145°) have reduced OASPL at all azimuthal angles with more reduction noted at azimuthal angle ϕ = 90°, where the observer sees the narrow side of the nozzle. There is a small polar angle range 110° < θ < 140° where the wide side is very slightly amplified over the round jet. By azimuthal angle ϕ = 60° the rectangular jet is quieter than the reference round jet at these aft angles, but has increases in the forward angles.

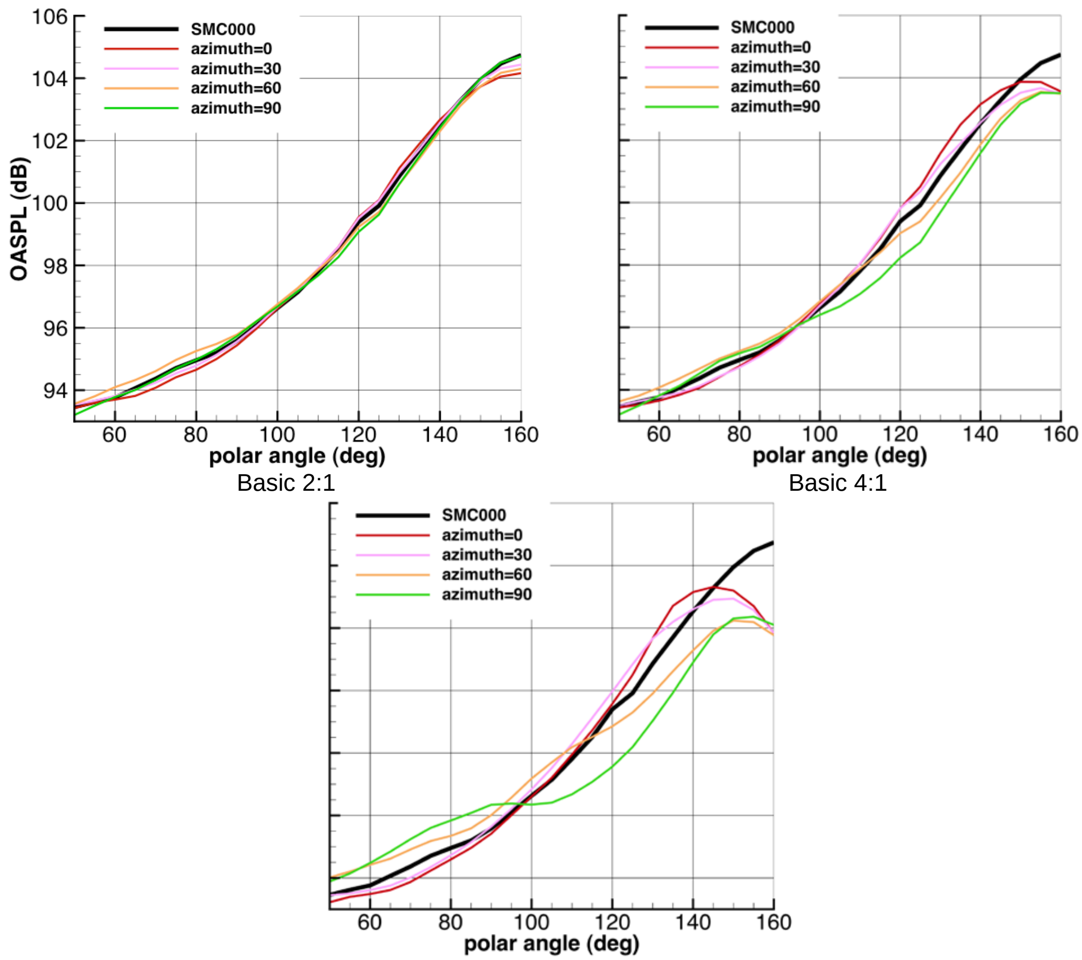


Figure 5.—OASPL directivity for basic rectangular nozzles at setpoint 7 (unheated, *Ma* = 0.9). Polar angle directivities for different aspect ratios are shown in each plot, with each line being different azimuthal angle. The black line is the reference round jet.

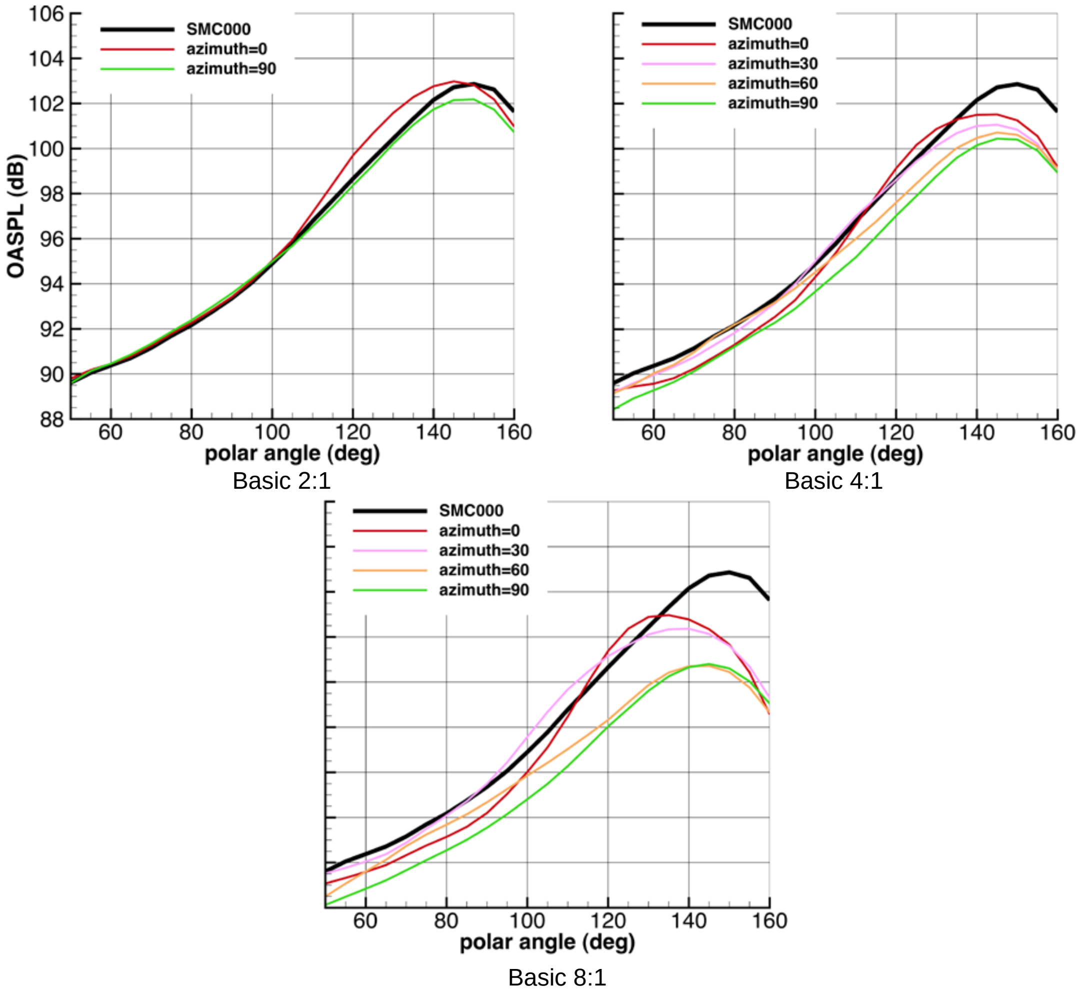


Figure 6.—OASPL directivity for basic rectangular nozzles at setpoint 46 ($T_j/T_\infty$ = 2.7, *Ma* = 0.9). Polar angle directivities for different aspect ratios are shown in each plot, with each line being different azimuthal angle. The black line is the reference round jet.

When the jet is heated many of the trends stay the same, but the rectangular nozzles are quieter relative to the round jet at forward angles. The rectangular jets exhibit even less noise than the round jet at the far aft angles than they did with cold flow. Figure 6 gives OASPL directivities for a hot jet condition with the same velocity as the cold jets shown in Figure 5 but now with a static temperature ratio of 2.7.

To better understand the origin of the OASPL changes, Figure 7 gives the spectra for the basic 8:1 nozzle at setpoint 7. In the plots the spectra at polar angles 90° and 150° are similar to the reference nozzle spectra, with the characteristic broadside and aft spectral shapes, with the θ = 150° data having a reduced peak relative to the round nozzle. So the aft angle reduction is a reduction in peak frequency jet noise. However, at polar angle θ = 120° there is substantial change in the directivity relative to the round jet, with the ϕ = 0° spectrum being similar to the spectral shape of the round jet broadside (θ = 90°), and the ϕ = 90° data being similar in spectral shape to the aft polar angle spectra. Perhaps one way to view it is that the rectangular jet has a shift in the polar angle at which the aft-angle spectra dominates the broadside spectrum. This shift is azimuthally dependent, with the wide side of the nozzle having the least aft-angle contribution.

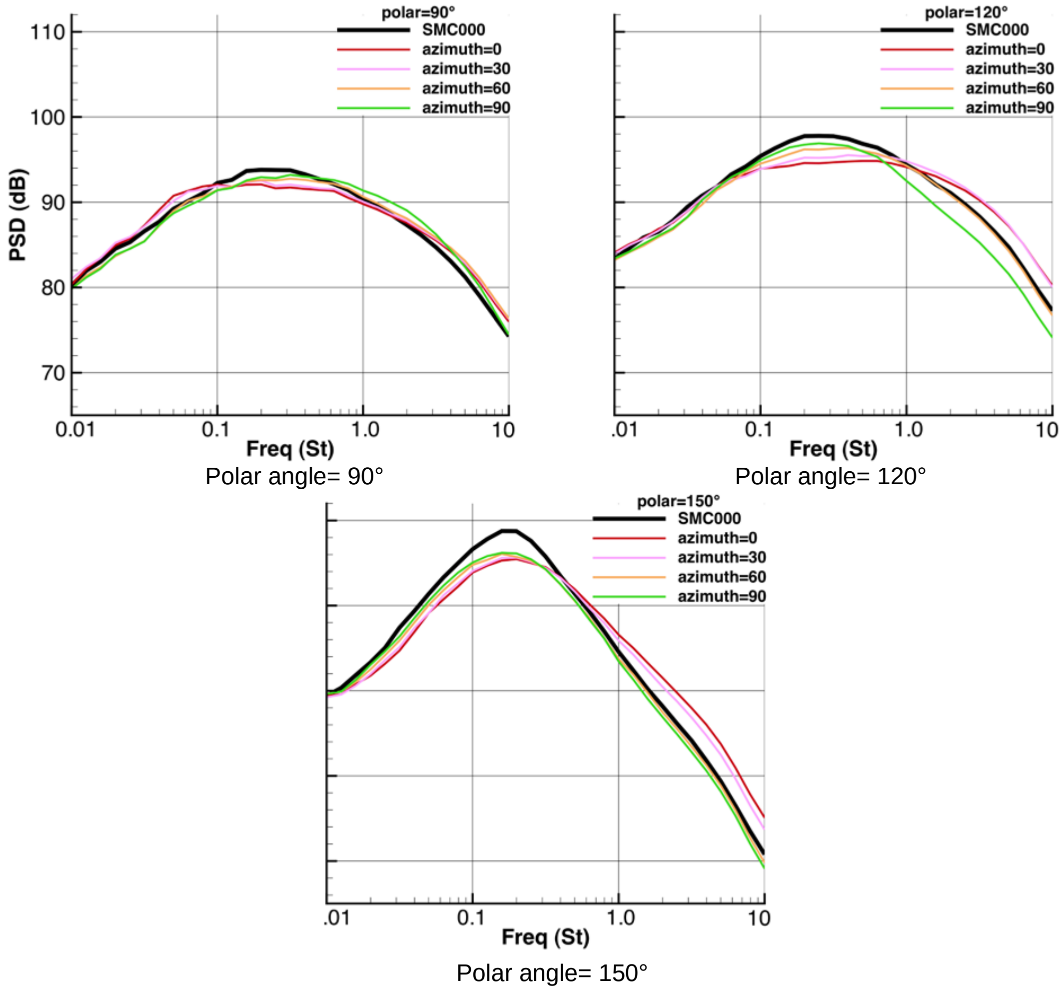


Figure 7.—Power spectral density for the basic 8:1 nozzle at three polar angles (90°, 120°, 150°) and several azimuthal angles for setpoint 7 (unheated, *Ma* = 0.9).

Turning now to the beveled nozzles, the OASPL directivities for the six beveled rectangular nozzles are shown in Figure 8. In the figure, plots show how the different azimuthal angles compare to a round reference nozzle (SMC000) for different aspect ratios and bevel lengths. Immediately notable is that the beveled nozzles are almost uniformly louder than the reference nozzle. Compared with their basic, non-beveled counterparts the beveled nozzles are louder. Perhaps most unexpectedly, the sound fields are nearly the same on the long and short sides of the nozzle. Longer bevel lengths are louder than short ones. The peak in the OASPL shifts substantially forward with bevel length. And while the narrow side observer ($\phi$ = 90°) is quieter at far aft polar angles ($\theta$ > 120°) on the long bevel lengths and high aspect ratios, there is a strong increase for this azimuthal angle for an observer broadside to the jet ($\theta$ ~ 90°).

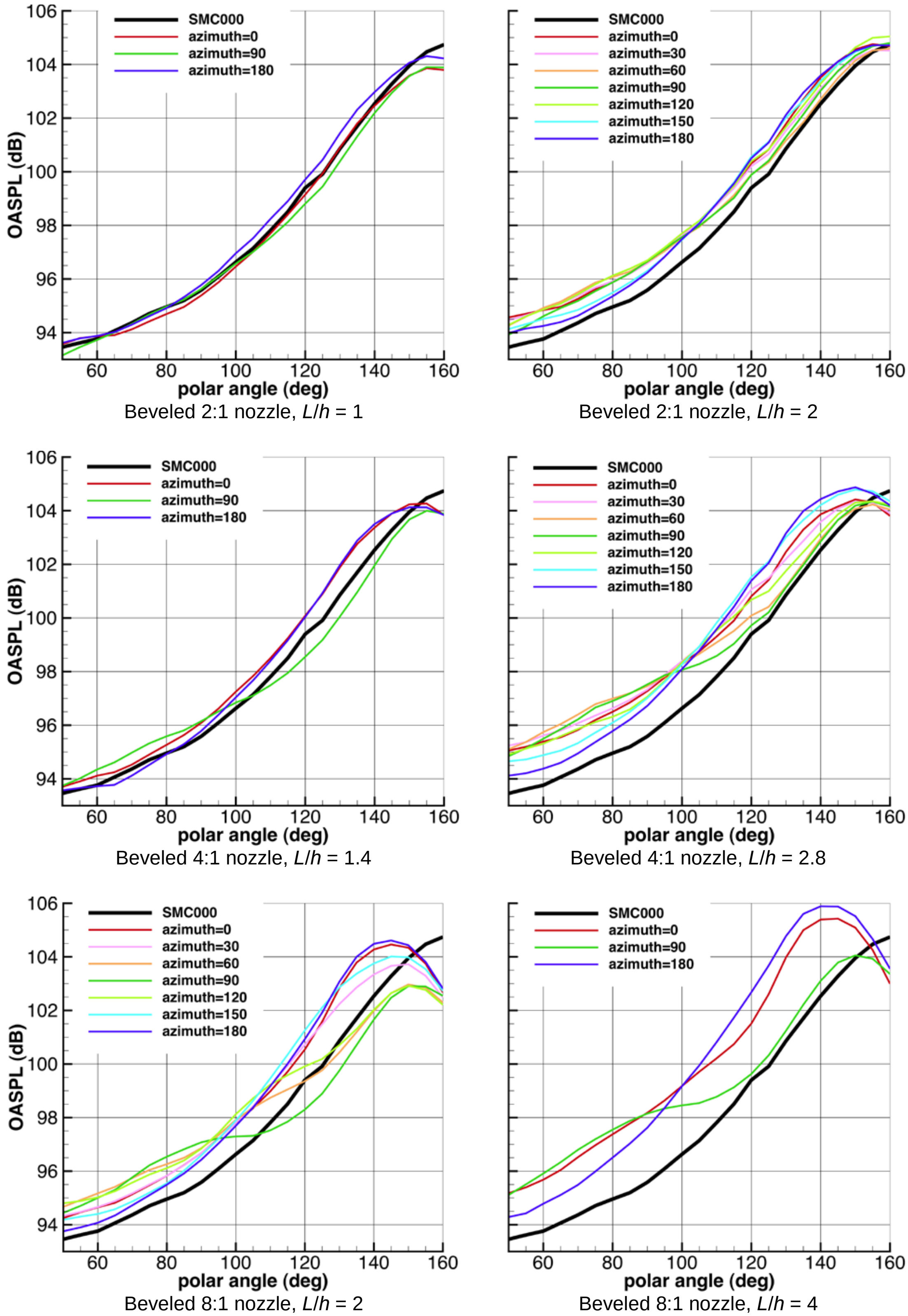


Figure 8.—OASPL directivity for beveled rectangular nozzles at setpoint 7 (unheated, *Ma* = 0.9). Polar angle directivities for different aspect ratios and bevel lengths are shown in each plot, with each line being different azimuthal angle. The black line is the reference round jet.

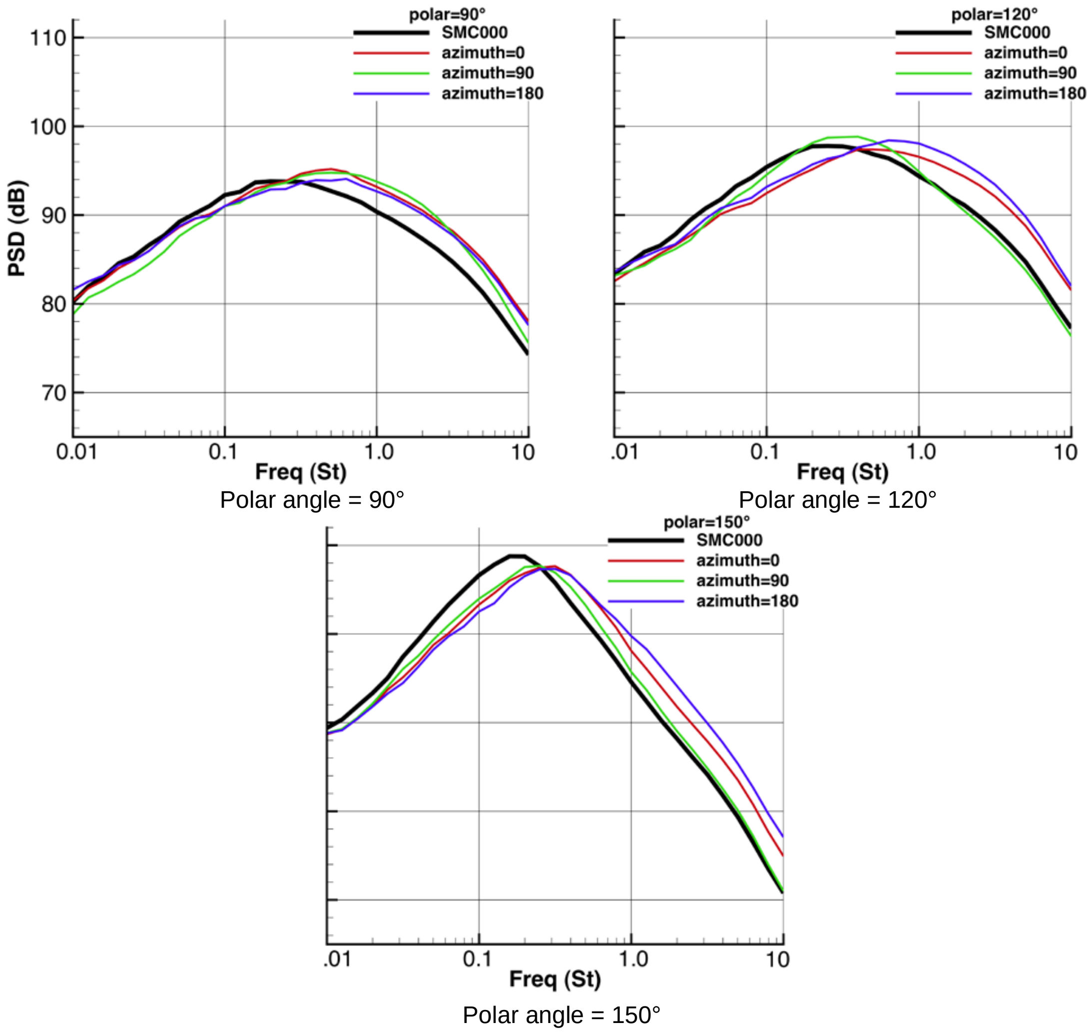


Figure 9.—Power spectral density for the long-beveled 8:1 nozzle at three polar angles (90°, 120°, 150°) and several azimuthal angles for setpoint 7 (unheated, *Ma* = 0.9).

Not shown here are configurations that were identical to the bevel nozzles but where the triangular sidewalls were removed, leaving just the long deck. These configurations had OASPL directivity immeasurably different from the bevel configurations presented here.

The spectral impact of the beveling is demonstrated for the 8:1 nozzle with the longest bevel (Figure 9). There is a substantial upward shift in the peak frequency even at polar angle θ = 90° in the beveled nozzle spectra. Rather than a changeover from broadside to aft spectral shapes, the difference at θ = 120° are less a change in shape than a change in peak frequency. And even at the spectral level of detail the short and long sides of the nozzle have nearly identical spectra.

## 3.2 Comparison With Historical Data

Data from the GTRI Reference 3 (Figure 9 to Figure 12, *Ma* = 0.9) were scanned and renormalized accounting for observer distance (10 ft arc in (Ref. 3) to 100$D_e$) and for the scaling with velocity and geometric dimension (*h* in (Ref. 3) to $D_e$) applied by the authors. The effects of atmospheric attenuation were assumed minimal and not addressed in the GTRI data. The present data were then overlaid on it as shown in Figure 10 for polar angle of θ = 90° (the NASA 2:1 nozzle was overlaid on the GTRI 1.5:1 nozzle). The comparison of round jet spectra is quite reasonable, being within 1 dB on third octave basis

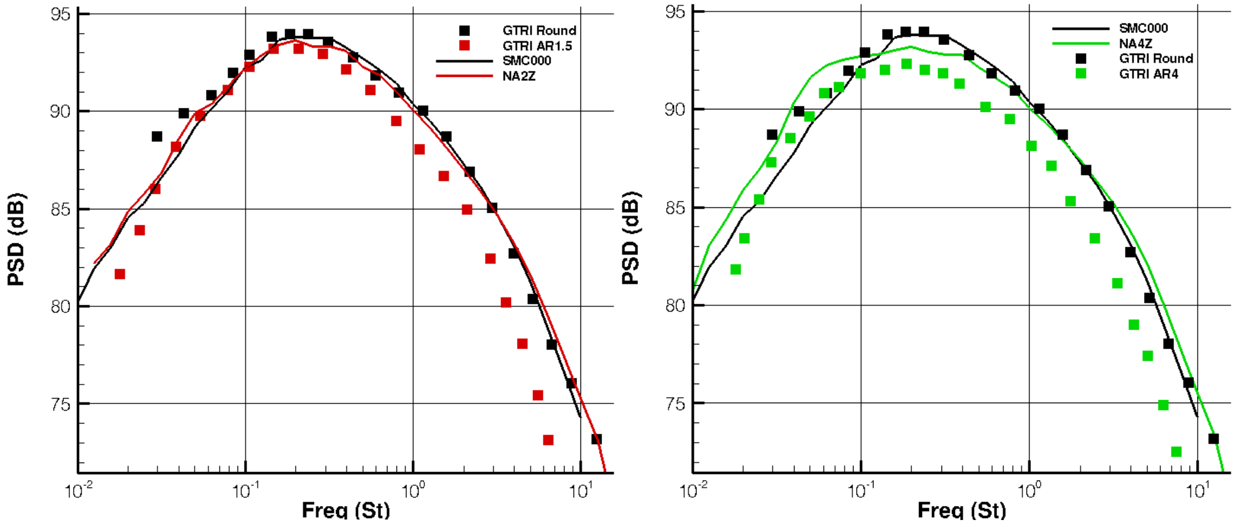


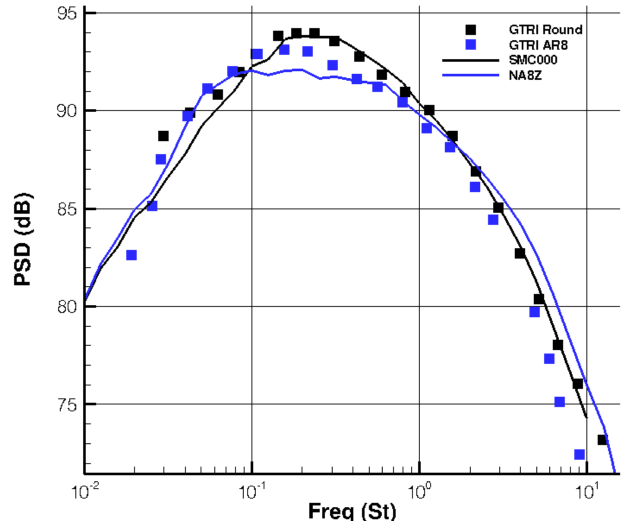


| GTRI Nozzle | Width, in. (mm) | Height, in. (mm) |
|---|---|---|
| Round Nozzle | 1.6 (40.64) | |
| Aspect Ratio 1.5 | 1.732 (43.99) | 1.155 (29.34) |
| Aspect Ratio 4.0 | 2.828 (71.83) | 0.707 (17.96) |
| Aspect Ratio 8.0 | 4.00 (101.6) | 0.500 (12.70) |

Figure 10.—Comparison of NASA data with that of GTRI (Ref. 3). Power spectral density at polar angle $\theta$ =90°, azimuthal angle $\phi$ = 0° for round and rectangular jets at three aspect ratios. Solid lines: NASA, squares: GTRI.

for all but the lowest frequencies. However, the GTRI data shows significant reduction for rectangular jets at *AR*=1.5 and 4 that the NASA experiments do not. This is especially critical in the high frequencies where NASA experiments show a slight increase and where noise typically has a strong contribution to the noy scaling of human hearing at full scale. More disturbing is that the GTRI data show the trend that *AR* = 4 is quieter than *AR* 1.5 or 8, whereas the NASA data monotonically trends to increasing noise reduction with increasing aspect ratio. Two general trends are found in common between NASA and GTRI datasets: reduction of noise at peak frequency, and increase of noise at frequencies below the peak with increasing aspect ratio. Other trends observed in (Ref. 3) are also evident in the NASA data, such as the shift in peak frequency at aft angles between wide and narrow-side observers (see Figure 7).

## 3.3 Modeling the Effect of Aspect Ratio and Bevel Length

### 3.3.1 Model for Impact of Nozzle Geometry on Spectral Directivity

After considerable examination of all the datasets, it was decided that the variations in spectral directivity were consistent enough to allow a low-order fit to the data in the parameters of aspect ratio and bevel length. This was first attempted for setpoint 7, the cold flow at *Ma* = 0.9.

Consider the parametric model for effect of Aspect Ratio (*AR*) and Bevel Length (*L*/*h*):

$$PSD(AR, L/h; f, \theta, \phi) = PSD0(f, \theta) + AR * a(f, \theta, \phi) + L/h * b(f, \theta, \phi) + AR * L/h * c(f, \theta, \phi)$$

The parametric model is a simple bilinear model for impact of aspect ratio (coefficient *a*) and bevel length (*b*) with one cross term (*c*). Counting the basic rectangular nozzles as bevel length $L = 0$ there are three aspect ratios and three lengths, a combination of nine data points from which to determine the coefficients *a, b,* and *c*. A singular value decomposition routine was employed to fit the equation to the data for each frequency, polar angle, and azimuthal angle. After some experience with looking at the resulting coefficients, it was determined that the constant *PSD*0 could be prescribed to be the spectral directivity of an equivalent round jet, making the model more robust. The results from the fitting after prescribing *PSD*0 in this manner are given in Figure 11 to Figure 14 for each coefficient and for the chi-squared value of the fit. In each figure three carpet plots are shown, one each for azimuthal angles 0°, 90°, and 180°. Each carpet plot gives power spectral density as a function of polar angle and frequency (given in Strouhal number based on equivalent diameter and ideally expanded velocity). The shape of the carpet plot is that of *PSD*0($f$,θ), and thus does not change from plot to plot. The color mapped onto this surface is the value of the coefficient named in that figure.

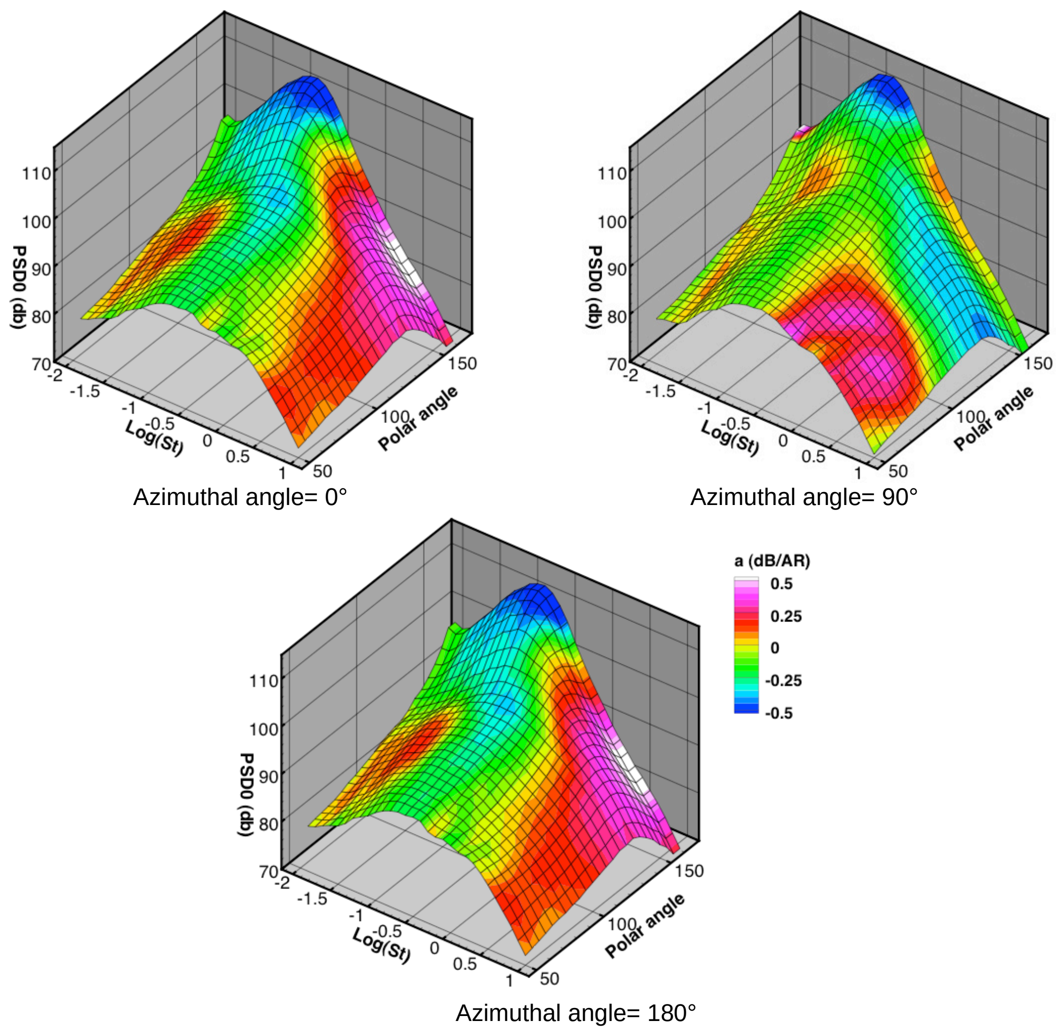


Figure 11.—Sensitivity of jet noise to aspect ratio: $a(f,\theta)$ for three values of azimuthal angles: $\phi$ = 0°, 90°, 180°.

Figure 11 shows the coefficient $a(f,\theta,\phi)$ for the cold, *Ma* = 0.9 jet flow. The color mapping shows positive values at high frequencies and negative values for the peak frequency at aft angles. This being the sensitivity of noise to aspect ratio, the color mapping quantifies how high frequency noise is increased with increase in aspect ratio while peak aft noise is decreased. Note that the trends are very similar for $\phi = 0°$ and 180°, but differ in polar angle at $\phi = 90°$, as was noted above in looking at the spectra in isolation.

Turning to sensitivity to bevel length, Figure 12 presents a similar set of plots for the coefficient $b(f,\theta,\phi)$. Note that all colors are orange-red, indicating only positive values for almost all frequencies and polar angles. Lengthening the bevel increases noise everywhere. There is a slight lessening of the increase with length in the forward direction, possibly a slight impact of the lower lip shielding the noise from the upper shear layer. However, the net effect of increasing bevel length is to increase the noise everywhere.

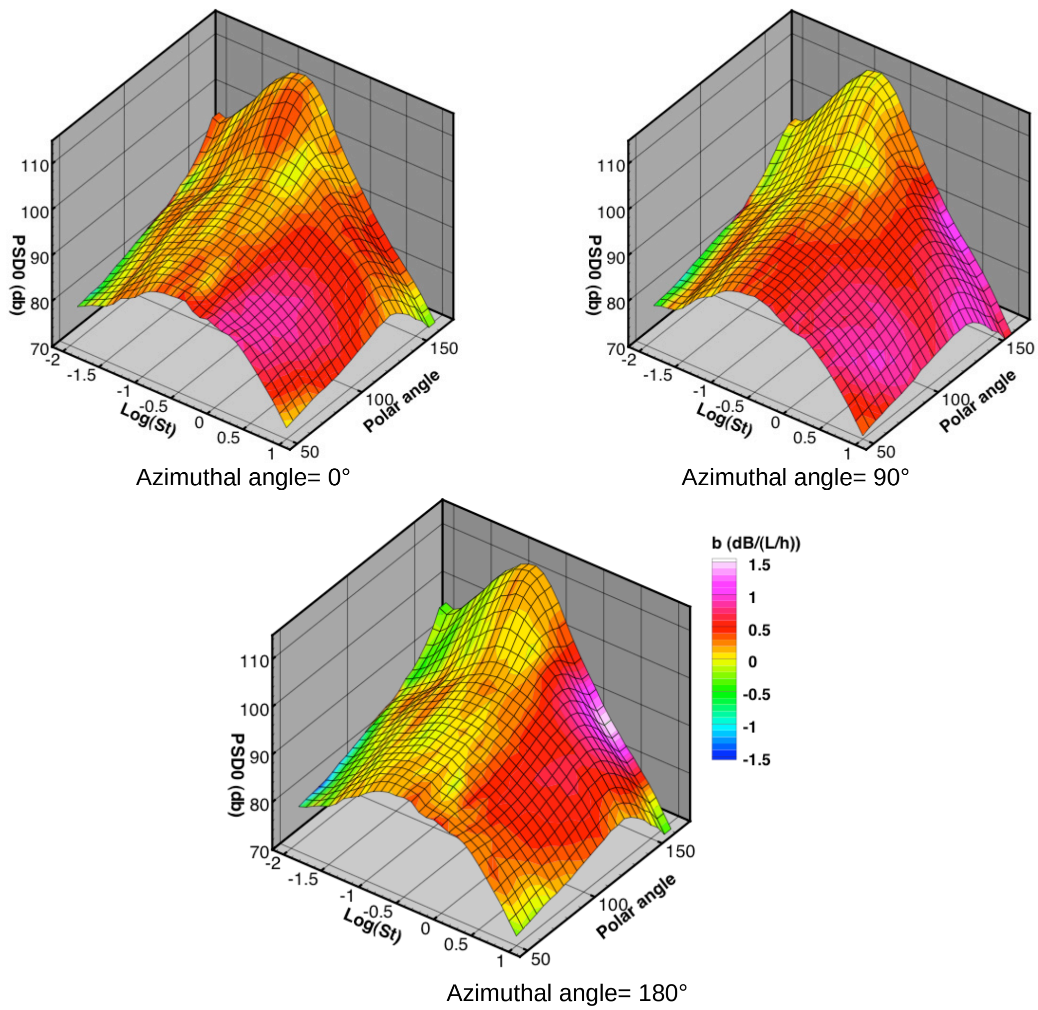


Figure 12.—Sensitivity of jet noise to bevel length: $b(f,\theta)$ for three azimuthal angles.

The cross-sensitivity coefficient (Figure 13) is largely neutral, indicating that aspect ratio and bevel length operate with surprising independence.

Finally, Figure 14 presents the chi-square value for the fit. These values represent the measure of the hypothesis that the difference in modeled and measured values is experimental error, with 5 degrees of freedom (nine data points, four coefficients). The values being much less than the critical chi-square value of 11.07 for a 95 percent confidence level at all frequencies and angles indicate that this simple model is a very good fit to the data.

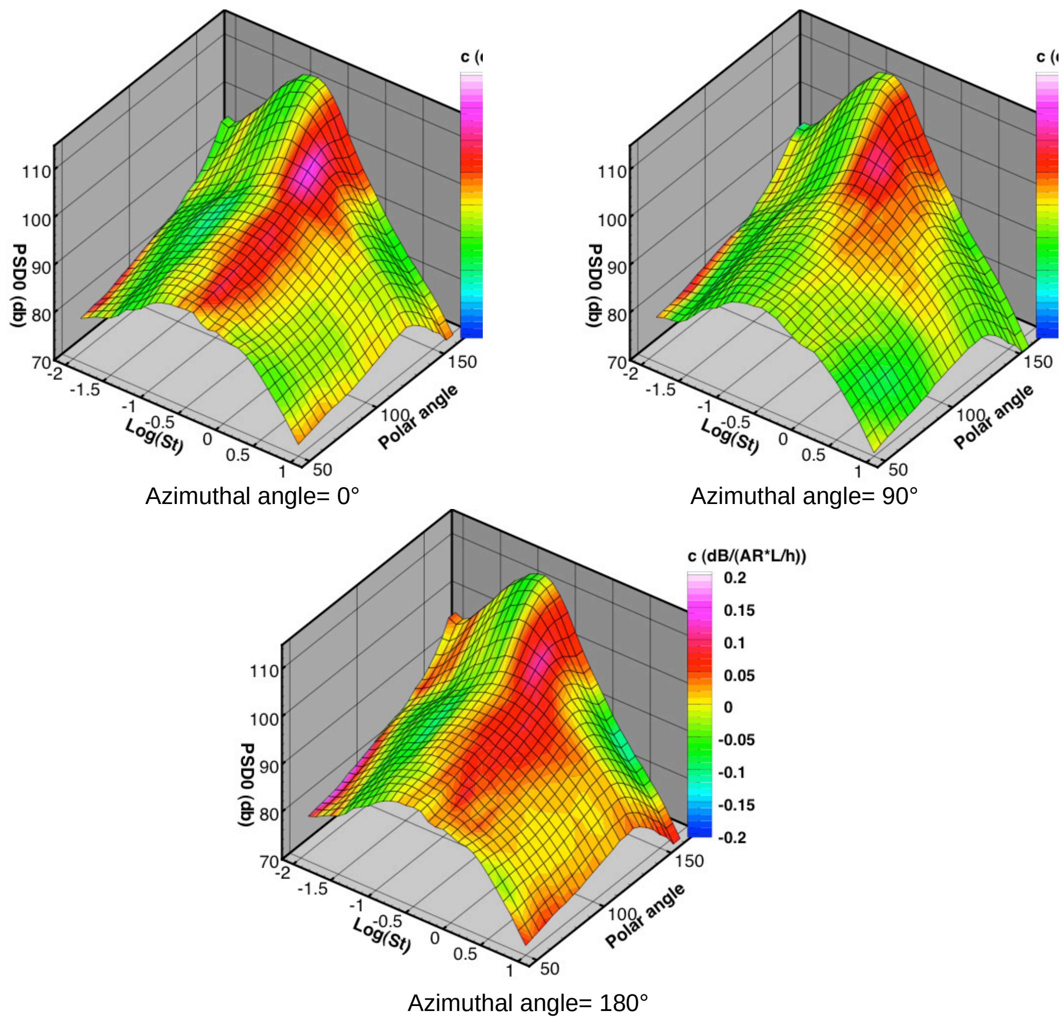


Figure 13.—Cross-sensitivity of jet noise to aspect ratio and bevel length: $c(f,\theta)$ for three azimuthal angles.

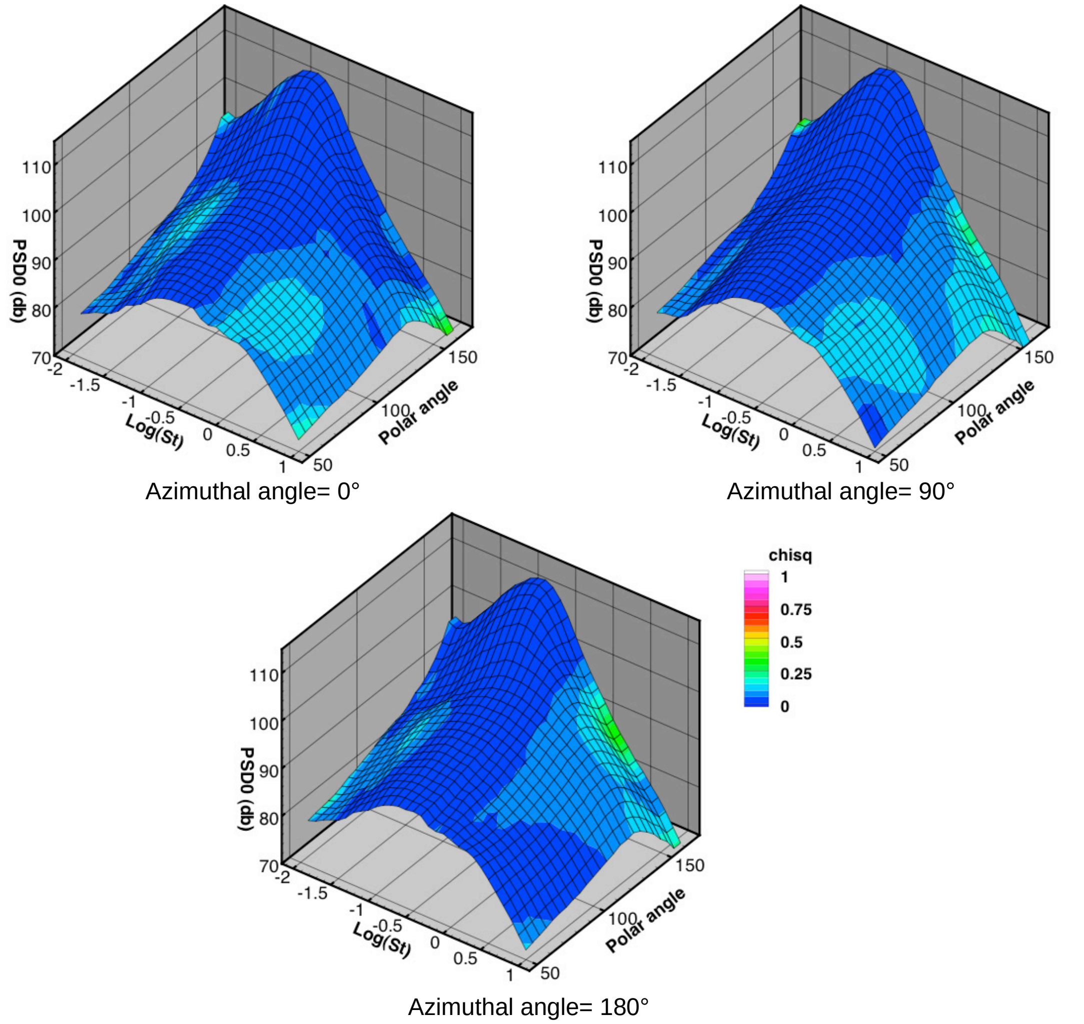


Figure 14.—Chi-squared goodness of fit for fitted model for jet noise *PSD*(*f*,θ) for three azimuthal angles.

### 3.3.2 Applicability of Spectral Directivity Model to Other Subsonic Flow Conditions

The model for far-field spectral directivity described above was developed using the cold, *Ma* = 0.9 jet noise data. This model uses either data or predicted spectral directivity of a round jet as its zeroth-order term (*PSD*0) and primarily describes the effect of aspect ratio and bevel length on the far-field noise. This was chosen with the idea that the large effects of jet condition, primarily velocity and temperature (density) could be accounted for by using an appropriate round jet spectral directivity, and the same coefficients for geometric effects.

To test this idea, the model was applied to several other flow conditions and compared with data acquired at those conditions. Specifically, the model was applied to setpoints 3, 23, and 46 (see Table 2) and compared with the measured far-field directivities. Representative predictions for three of these flow conditions are shown in Figure 15 as carpet plots of spectral directivity. The discrepancy, in ΔdB (model – data), is shown by the colors painted on the surface. The model worked well for the aspect ratio 2:1, *Ma* = 0.5, warm jet, with discrepancies being less than 1 dB (mostly much less) for all angles and frequencies. This was not surprising given that there is little variation with nozzle geometry at this aspect ratio and the *PSD*0 term from the round jet accounts for most of the prediction. The model fared worse as the aspect ratio effect increased and temperature ratio increased. The model does not credit the geometric

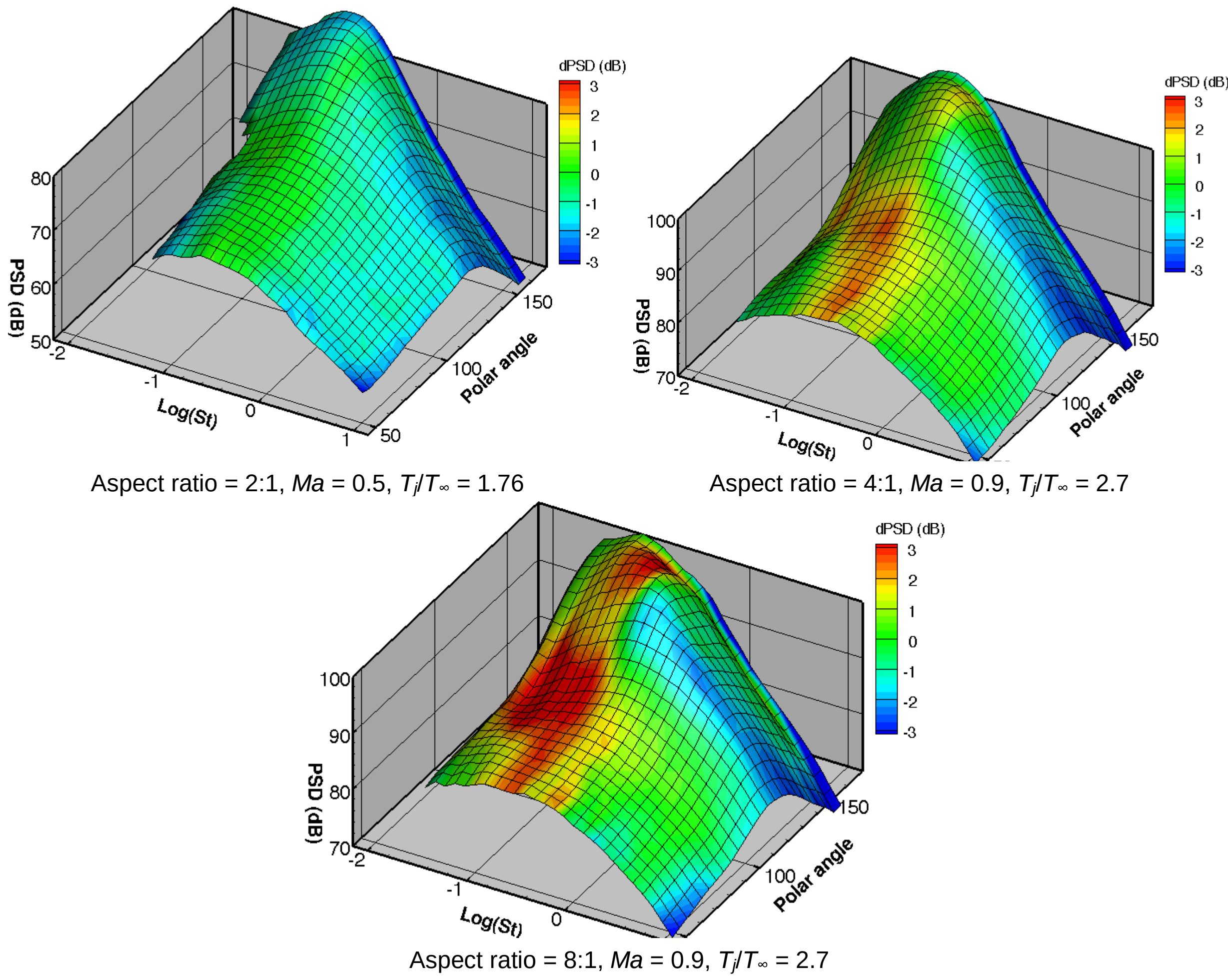


Figure 15.—Error in predicting hot jets with model derived for cold, *Ma* = 0.9 jet data. Surface height gives predicted spectral directivity, colors give difference in dB (model – data). Three flow conditions shown, all at azimuthal angle $\phi = 0°$.

difference with as much benefit as the data shows (ΔdB, model – data, positive) at polar angles broadside to the jet. The model also predicts more high frequency reduction relative to the round jet at the far aft angles than the data shows. This discrepancy is magnified at the larger aspect ratio of 8:1.

To summarize the performance of the model for all hot jets, a metric was constructed that would encompass the error over all angles and frequencies. The metric used was the root-mean-square of the difference between the model and data in dB. The difference, in dB, for each flow condition and geometric variation was squared, integrated over frequency and polar angle, and its square root taken. These integrated measures of the error of the model are presented in Figure 16, plotted in the parameter space of aspect ratio, bevel length ($L/h$), and Mach number *Ma*. The locations of the spheres give the parameters of the flow and geometry while the size give the magnitude of the error. Quantitatively, the magnitude of the error can be read from the color of the spheres and the corresponding colored bar. Generally speaking, the rms error of the model is much less than 1 dB for cold flows, increasing to 1 to 2 dB for the hot flows. The long bevel, 8:1 nozzle at *Ma* = 0.5 is a standout, the data having a strong peak frequency to the observer at azimuthal angle $\phi = 0°$ (wide side of the nozzle) which is not captured by the model. More investigation of this anomaly is required.

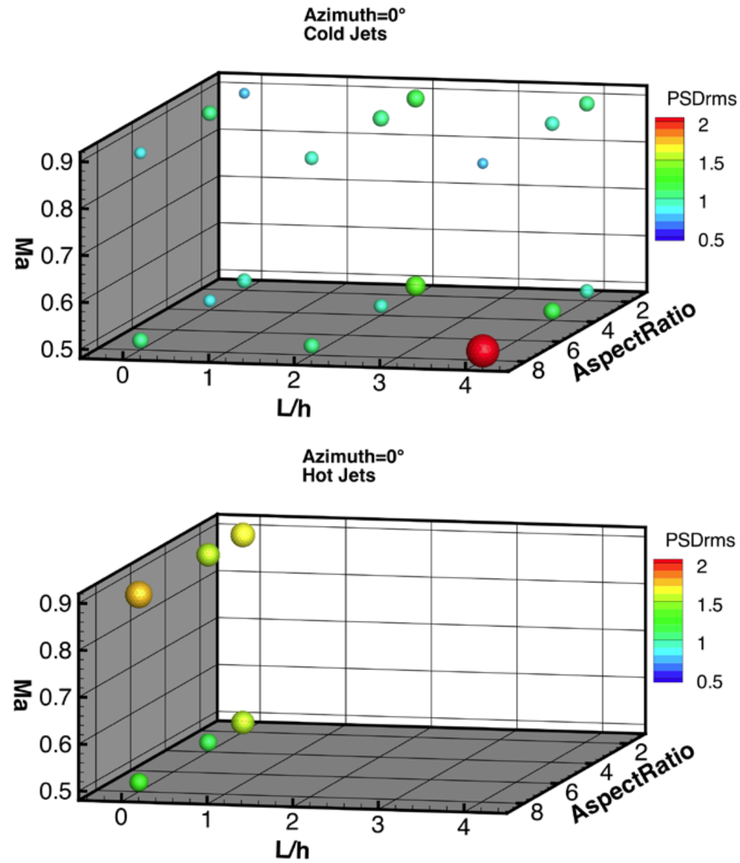


Figure 16.—Error of model applied to different jet flow conditions. Root-mean-square of difference in spectral directivity between model developed for cold, *Ma* = 0.9 and data at other conditions. Unheated jets (left), heated jets (right).

## 4.0 Discussion

One of the main changes in spectral directivity caused by the nozzle increasing aspect ratio is the azimuthal dependence of the polar angle where broadside noise spectra change to aft noise spectra. This is very clear when looking at spectra at polar angle $\theta = 120°$ where the broadside shape describes the spectra seen by an observer on the wide side of the nozzle while the aft shape describes the spectra seen by an observer on the narrow side of the nozzle. Depending upon the what jet noise theory one subscribes to this could be caused by differences in the balance of large and small-scale sources directed in the two planes or by differences in the propagation of the noise due to the differences in shear layer spreading on the two sides of the plume.

From an engineering perspective it is disappointing not to find as much noise reduction in the rectangular nozzles as has previously been found in (Ref. 3). Care was taken in rescaling the data from the GTRI paper, and the agreement of the round jet data between that paper and the present test partially validates the calculations. Assuming that renormalization of data was done accurately, the next best guess for the discrepancy would be the possibility of nonuniform exit profiles from the round-to-rectangular transition of the GTRI nozzles. Anecdotally, this has been found to produce differences in the noise of elliptic jets, an issue that was carefully addressed in the current design to produce a uniform exit profile for the NASA rectangular nozzles (Ref. 1). If nonuniformity were the cause of the discrepancy, then clearly the next task is to find the proper nonuniformity to lower the jet noise.

The biggest surprise of the modeling effort described in Section 3.3 was that such a simple model fit the data so well, at least for cold jets. There may be a need to incorporate some additional impact of aspect ratio when the jet is heated, as these effects were underpredicted for the hot flows tested. There is also a need to acquire hot jet data for bevel nozzles to assess whether the geometric model for bevel length holds for hot jets as well as it does for cold jets. Using a more physics-based modeling approach should improve this model over the full range of flow conditions.

## 5.0 Summary

Rectangular nozzles of aspect ratio 2:1, 4:1, and 8:1 were constructed with care to assure that the exit velocity profile was uniform after the round to rectangular transition and contraction. Extending the wide edge of one side to create beveled nozzles created additional nozzles with the same contraction. The nozzles were tested acoustically over a wide but sparse range of flow conditions, mapping out the spectral directivity of the noise from the nozzles. For high subsonic flow conditions several trends were observed, mostly showing an upstream shift in peak aft noise with increasing aspect ratio and an increase in high frequency noise for observers broadside to the jet. Azimuthally, there was generally noise reduction for observers on the narrow side of the nozzle, but an increase for observers on the wide side. With extended bevel length, the noise increased everywhere. These trends were confirmed by fitting a simple bilinear polynomial to the dataset, isolating the sensitivity to aspect ratio and bevel length for each observer angle. This fit quantifies these trends and allows for a simple empirical model for the noise of rectangular jets relative to round jets.

## References


1. Frate, F.C. and Bridges, J., “Extensible Rectangular Nozzle Model System,” AIAA–2011–0975, January 2011.
2. Balsa, T.F., Gliebe, P.R., Kantola, R.A., Mani, R., Stringas, E.J., and Want, F.C.F., “High Velocity Jet Noise Source Location and Reduction: Task 2 – Theoretical Developments And Basic Experiments,” FAA-RD-76-79, May 1978.
3. Massey, K.C., Ahuja, K.K., and Gaeta, R., “Noise Scaling for Unheated Low Aspect Ratio Rectangular Jets,” AIAA Paper 2004-2946, May 2004.
4. Viswanathan. K. “Jet aeroacoustic testing: issues and implications,” AIAA J 41, 1674 (2003).
5. Ahuja. K.K., “Designing clean jet-noise facilities and making accurate jet-noise measurements,” Intl J. Aeroacoustics 2, 314 (2003).
6. Brown, C.A., & Bridges, J., “Small Hot Jet Acoustic Rig Validation,” NASA TM—2006/214234 (2006).
7. Tanna, H.K, Dean, P.D, Fisher, M.J, “The Influence of Temperature on Shock-Free Supersonic Jet Noise”, *J. Sound Vib.*, Vol. 39(4), 1975, pp. 429-460.
8. Shields, F. D. and Bass, H. E., “Atmospheric Absorption of High Frequency Noise and Application to Fractional- Octave Band,” NASA-CR 2760, (1977).

| REPORT DOCUMENTATION PAGE | *Form Approved OMB No. 0704-0188* |
|---|---|



**1. REPORT DATE** *(DD-MM-YYYY)*
01-08-2012

**2. REPORT TYPE**
Technical Memorandum

**3. DATES COVERED** *(From - To)*

**4. TITLE AND SUBTITLE**
Acoustic Measurements of Rectangular Nozzles With Bevel

**5a. CONTRACT NUMBER**

**5b. GRANT NUMBER**

**5c. PROGRAM ELEMENT NUMBER**

**6. AUTHOR(S)**
Bridges, James, E.

**5d. PROJECT NUMBER**

**5e. TASK NUMBER**

**5f. WORK UNIT NUMBER**
WBS 984754.02.07.03.17.08

**7. PERFORMING ORGANIZATION NAME(S) AND ADDRESS(ES)**
National Aeronautics and Space Administration
John H. Glenn Research Center at Lewis Field
Cleveland, Ohio 44135-3191

**8. PERFORMING ORGANIZATION REPORT NUMBER**
E-18349

**9. SPONSORING/MONITORING AGENCY NAME(S) AND ADDRESS(ES)**
National Aeronautics and Space Administration
Washington, DC 20546-0001

**10. SPONSORING/MONITOR'S ACRONYM(S)**
NASA

**11. SPONSORING/MONITORING REPORT NUMBER**
NASA/TM-2012-217674

**12. DISTRIBUTION/AVAILABILITY STATEMENT**
Unclassified-Unlimited
Subject Categories: 34 and 71
Available electronically at http://www.sti.nasa.gov
This publication is available from the NASA Center for AeroSpace Information, 443-757-5802

**13. SUPPLEMENTARY NOTES**

**14. ABSTRACT**
A series of convergent rectangular nozzles of aspect ratios 2:1, 4:1, and 8:1 were constructed with uniform exit velocity profiles. Additional nozzles were constructed that extended the wide lip on one side of these nozzles to form beveled nozzles. Far-field acoustic measurements were made and analyzed, and the results presented. The impact of aspect ratio on jet noise was similar to that of enhanced mixing devices: reduction in aft, peak frequency noise with an increase in broadside, high frequency noise. Azimuthally, it was found that rectangular jets produced more noise directed away from their wide sides than from their narrow sides. The azimuthal dependence decreased at aft angles where noise decreased. The effect of temperature, keeping acoustic Mach number constant, was minimal. Since most installations would have the observer on the wide size of the nozzle, the increased high frequency noise has a deleterious impact on the observer. Extending one wide side of the rectangular nozzle, evocative of an aft deck in an installed propulsion system, increased the noise of the jet with increasing length. The impact of both aspect ratio and bevel length were relatively well behaved, allowing a simple bilinear model to be constructed relative to a simple round jet.

**15. SUBJECT TERMS**
Airport noise; Jet noise; Aeroacoustics; Large eddy simulation; Supersonic aircraft; Embedded propulsion

| 16. SECURITY CLASSIFICATION OF: | | | 17. LIMITATION OF ABSTRACT | 18. NUMBER OF PAGES | 19a. NAME OF RESPONSIBLE PERSON |
|---|---|---|---|---|---|
| | | | | | STI Help Desk (email:help@sti.nasa.gov) |
| **a. REPORT** | **b. ABSTRACT** | **c. THIS PAGE** | | | **19b. TELEPHONE NUMBER** *(include area code)* |
| U | U | U | UU | 26 | 443-757-5802 |

Standard Form 298 (Rev. 8-98)
Prescribed by ANSI Std. Z39-18